J|A|C|S
COMMUNICATIONS

Published on Web 11/21/2003

Controlling Diaza-Cope Rearrangement Reactions with Resonance-Assisted Hydrogen Bonds

Jik Chin,* Fabrizio Mancin, Nirusha Thavarajah, Donghyung Lee, Alan Lough, and Doo Soo Chung*

Department of Chemistry, 80 St. George Street, Toronto M5S 3H6, Canada, and Department of Chemistry, Seoul National University, Seoul 151-747, Korea

Received September 27, 2003; E-mail: jchin@chem.utoronto.ca; dschung@snu.ac.kr

Over the years, hydrogen bonds have been the subject of great interest to chemists and biologists. Many weak forces of individual hydrogen bonds can add up to considerable strengths in large biomolecules such as nucleic acids and proteins. There has been much recent interest in short, strong hydrogen bonds and their potential role in chemical and enzymic reactions.[1−5] Seminal work by Gilli et al. has shown the existence of a class of unusually short, strong hydrogen bonds they termed resonance-assisted hydrogen bonds (RAHBs).[6,7] It has been generally difficult to demonstrate large effects in chemical reactions with short strong hydrogen bonds. In a series of elegant studies, Vögtle et al.[8−10] showed that the equilibrium for the [3,3]-sigmatropic shift reaction favors the formation of **1** over **2** (Scheme 1).

Scheme 1

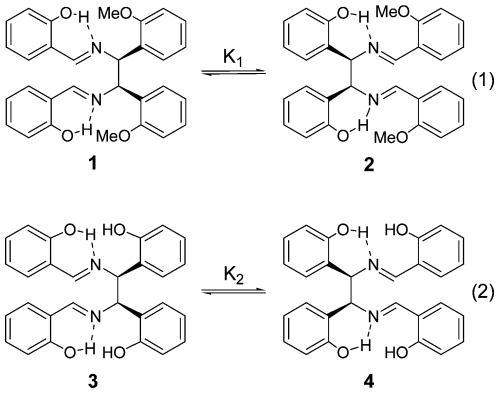

Although it was suspected that internal hydrogen bonds (H-bonds) may play a role in the selectivity,[9] it was not known how much this would affect the equilibrium since both **1** and **2** can form internal H-bonds. Our interest in H-bonds[11,12] led us to investigate the origin of this selectivity. Here we report crystal, ^{1}H NMR, and DFT computational data for **1**, **2**, and **3** and the role of RAHBs on diaza-Cope rearrangement reactions.

The intramolecular H-bonds in salicyl imines (**5**) have been thoroughly characterized as RAHBs on the basis of crystal, NMR, IR, and computational data.[14,15] In RAHBs, the H-bond is strengthened by π-delocalization (**5**). The N···O distances in these compounds ($2.65 > d(\mathrm{N\cdots O}) > 2.48$ Å) are significantly shorter than those in normal H-bonds. In addition, the ^{1}H NMR signals of the strongly H-bonded protons are highly downfield-shifted ($13 < \delta_{NH} < 18$ ppm). DFT computation at the B3LYP/6-31+G(d,p) level showed that the RAHBs (5 kcal/mol) are worth about twice the energy of normal H-bonds (2.5 kcal/mol). Thus, RAHBs are clear examples of short, strong H-bonds.

Compounds **1**, **2**, and **3** were prepared following the procedures in the literature.[8] X-ray quality crystals were obtained by recrystallization from chloroform/methanol (**1** and **2**) or DMSO/water

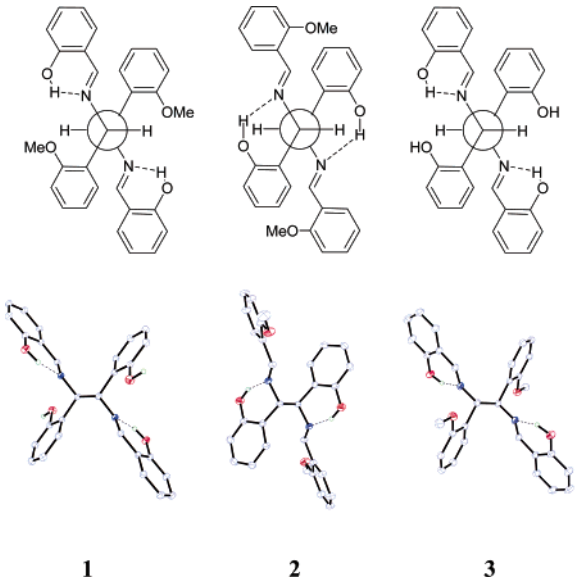

Figure 1. Crystal structures of **1**, **2**, and **3** with corresponding reprensentations on top.

Chart 1

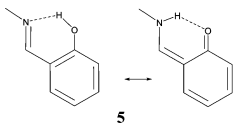

(**3**).[13] Crystallographic studies show that there are two internal H-bonds for each of the compounds **1**, **2**, and **3** (Figure 1). However, the two H-bonds in **1** are quite different in character from the two in **2**. The two H-bonds in **1** are RAHBs, whereas the two in **2** are normal H-bonds. Compound **3** could, in principle, form either two internal RAHBs or normal H-bonds. Crystal structure reveals that in solid-state compound **3** forms the more stable RAHBs in agreement with the above computation.

It should be pointed out that the H-bond distances of **1** and **3** are only slightly shorter than those in **2**. The N···H distances in **1** and **3** are 1.66 and 1.73 Å, respectively, while the two in **2** are 1.75 Å. The N···O distances in **1**, **2**, and **3** are 2.61, 2.64, and 2.62 Å, respectively. The C−N bonds involved in RAHBs are expected to be longer than usual due to the resonance effect (**5**), and the phenolic O−C bond distances involved in RAHBs are expected to be shorter (**5**).[14] Indeed, the imine C−N distances are longer in **1** (1.284) and **3** (1.288) than in **2** (1.276), and the phenolic O−C bond distances are shorter in **1** (1.357) and **3** (1.359) than in **2** (1.376). Interestingly, the crystal structures of **1** and **3** are virtually superimposable (Figure 1 and Chart 1). Even the crystal structure of **2** is quite closely related to those of **1** and **3**. All three structures are in fully staggered conformations about the central C−C bond

10.1021/ja0387554 CCC: $25.00

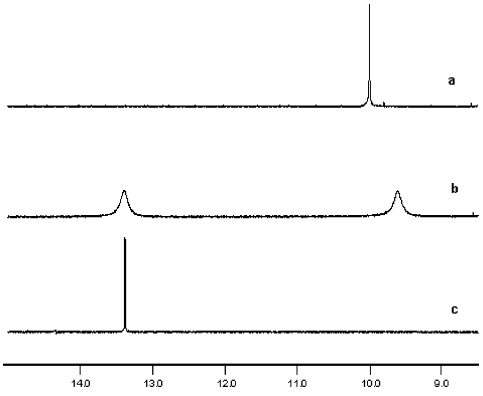

Figure 2. ^{1}H NMR of the phenolic protons in **1**, **2**, and **3**. The signal for the RAHB protons in **1** are downfield-shifted (c) relative to that for the regular H bonds in **2** (a). The chemical shift for the RAHB protons in **3** is about the same as that for **1** (the remaining phenolic proton signal that is not H-bonded appear slightly upfield of the H-bonded protons in **2**.

(Chart 1). The only major difference with structure **2** is that the methoxy phenyl groups are rotated about 180° relative to the hydroxy phenyl groups in **1** and **3** (Figure 1).

Figure 2 shows the ^{1}H NMR (d_6-DMSO) signals of the H-bonded protons in **1**, **2**, and **3**. The signal due to the H-bonded protons in **1** is downfield-shifted as expected for a RAHB. In contrast, the signal due to the H-bonded protons in **2** is in the normal H-bond range. The chemical shift due to the H-bonded protons in **3** matches the one for the H-bonded protons in **1**. The signals due to the two H-bonded protons in **2** are downfield-shifted relative to the signal due to the phenolic protons in **3** that are not H-bonded. Thus, the solution NMR data are in agreement with the solid-state data in that **1** and **3** form RAHBs.

In reaction 1 (Scheme 1), equilibrium can only be established through the sigmatropic shift reaction. In reaction 2, equilibrium can be established either through the sigmatropic shift reaction or simply through H-bond exchange. Equilibration of reaction 1 by sigmatropic shift rearrangement reaction gives **1** without any detectable amount of **2**, while equilibration of reaction 2 by H-bond exchange appears to give only **3**. The value of K_1 should be comparable to that of K_2 since the diaza-Cope rearrangement reaction is not highly sensitive to electronic effects and the electron-donating ability of a methoxy group approximates that of the hydroxy group. Each of the two RAHBs in **1** and **3** should be about 2.5 kcal/mol stronger than the two normal H-bonds in **2** and **4**.[14] Thus, **1** and **3** should be about 5 kcal/mol more stable than **2** and **4**, respectively, leading to K_1 and K_2 values of about 2.5×10^{-4} at 25 °C.

DFT computation at the B3LYP/6-31++G(d,p) level shows that **1** is about 6.62 kcal/mol more stable than **2** in reasonable agreement with the simple estimation above.[16] This translates to an amazing selectivity or K_1 value of 1.4×10^{-5}! Athough there may well be factors other than RAHBs (e.g., steric, electronic, etc.) that affect the relative stability of **1** and **2**, these effects appear to be small. Crystal structures of **1** and **2** were used as starting geometries for the geometry optimization calculations. The optimized structures are in good agreement with the crystal structures (root mean square displacement for **1**: 1.29 Å; for **2**: 0.30 Å).

Over the last several years, interesting papers on structures (crystal and spectroscopic data) and energetics (computational data) for RAHBs have appeared. However, effects of RAHB on chemical reactions have not been reported. Finding functional roles of RAHB is a challenge that may yield interesting results. In this communication, we have shown that RAHB is responsible for complete conversion of a class of sigmatropic shift reactions. Understanding how to control diaza-Cope rearrangement reactions with RAHBs may be useful for synthesizing a variety of 1,2-diamines, an important class of compounds for making catalysts and drugs.[17−20]

Acknowledgment. We thank the Natural Sciences and Engineering Research Council of Canada and the Center for Advanced Bioseparation Technology, and the BK21 program of Korea (D.L. and D.S.C.), for financial support of this work.

Supporting Information Available: Crystallographic data for **1**, **2**, and **3** (CIF) and their synthesis (PDF). This material is available free of charge via the Internet at http://pubs.acs.org.

References

(1) Cleland, W. W.; Kreevoy, M. M. *Science (Washington, DC)* **1994**, *264*, 1887−1890.
(2) Frey, P. A.; Whitt, S. A.; Tobin, J. B. *Science (Washington, DC)* **1994**, *264*, 1927−1930.
(3) Guthrie, J. P. *Chem. Biol.* **1996**, *3*, 163−170.
(4) Shan, S.-o.; Loh, S.; Herschlag, D. *Science (Washington, DC)* **1996**, *272*, 97−101.
(5) Warshel, A.; Papazyan, A.; Kollman, P. A. *Science (Washington, DC)* **1995**, *269*, 102−104.
(6) Gilli, G.; Bellucci, F.; Ferretti, V.; Bertolasi, V. *J. Am. Chem. Soc.* **1989**, *111*, 1023−1028.
(7) Bertolasi, V.; Gilli, P.; Ferretti, V.; Gilli, G. *J. Am. Chem. Soc.* **1991**, *113*, 4917−4925.
(8) Vögtle, F.; Goldschmitt, E. *Chem. Ber.* **1976**, *109*, 1−40.
(9) Vögtle, F.; Goldschmitt, E. *Angew. Chem., Int. Ed. Engl.* **1974**, *13*, 480.
(10) Vögtle, F.; Goldschmitt, E. *Angew. Chem., Int. Ed. Engl.* **1973**, *12*, 767.
(11) Chin, J.; Chung, S.; Kim, D. H. *J. Am. Chem. Soc.* **2002**, *124*, 10948−10949.
(12) Mancin, F.; Chin, J. *J. Am. Chem. Soc.* **2002**, *124*, 10946−10947.
(13) Crystal data for **1**: Monoclinic, *P*2(1)/*n*, $a = 12.5730(6)$ Å, $b = 6.6740(3)$ Å, $c = 14.6770(6)$ Å, $\alpha = 90°$, $\beta = 101.2780(18)°$, $\gamma = 90°$, $V = 1207.80(11)$ Å^3, $Z = 2$; Final *R* indices [$I > 2\sigma(I)$], R1 = 0.0428, wR2 = 0.1062; *R* indices (all data) R1 = 0.0616, wR2 = 0.1179. Crystal data for **2**: Triclinic, *P*-1, $a = 6.7660(3)$ Å, $b = 10.2215(4)$ Å, $c = 11.6018(6)$ Å, $\alpha = 108.690(2)°$, $\beta = 101.930(2)°$, $\gamma = 95.511(2)°$, $V = 732.15(6)$ Å^3, $Z = 1$; Final *R* indices [$I > 2\sigma(I)$], R1 = 0.0852, wR2 = 0.2136; *R* indices (all data) R1 = 0.1139, wR2 = 0.2328. Crystal data for **3**: Monoclinic, *P*2(1)/*c*, $a = 11.4887(4)$ Å, $b = 5.9506(2)$ Å, $c = 22.0286(7)$ Å, $\alpha = 90°$, $\beta = 93.419(2)°$, $\gamma = 90°$, $V = 1503.30(9)$ Å^3, $Z = 2$; Final *R* indices [$I > 2\sigma(I)$], R1 = 0.0489, wR2 = 0.1171; *R* indices (all data) R1 = 0.0717, wR2 = 0.1312.
(14) Gilli, P.; Bertolasi, V.; Ferretti, V.; Gilli, G. *J. Am. Chem. Soc.* **2000**, *124*, 10405−10417.
(15) Filarowski, A.; Koll, A.; Glowiak, T. *J. Chem. Soc., Perkin Trans. 2* **2002**, 835−842.
(16) All calculations used the *JAGUAR*, v4.1, quantum chemistry software. To calculate the geometries and energies, DFT, B3LYP, which includes generalized gradient approximation, and a component of the exact Hartree−Fock exchange, was used. This level of theory is combined with the basis set 6-31G(d,p) or 6-31G++(d,p). The 6-31G(d,p) was used to calculate the optimized geometry and vibrational frequencies, and then the 6-31++G(d,p) was used for single point energy (E_{0K}) calculation. We checked that all geometries were at the minima. The gas-phase Gibbs free energy is calculated as $\Delta G^0 = \mathrm{ZPE} + \Delta\Delta G_{0\rightarrow 298K} + E_{0K}$ Zero-point energy (ZPE) and Gibbs free energy change ($\Delta\Delta G_{0\rightarrow 298\ K}$) from 0 K to 298 K and at 1 atm were obtained form vibrational frequencies.
(17) Lucet, D.; Le Gall, T.; Mioskowski, C. *Angew. Chem., Int. Ed.* **1998**, *37*, 2580−2627.
(18) Bernhardt, G.; Gust, R.; Reile, H.; Vom Orde, H. D.; Mueller, R.; Keller, C.; Spruss, T.; Schoenenberger, H.; Burgemeister, T. *J. Cancer Res. Clin. Oncol.* **1992**, *118*, 201−208.
(19) Corey, E. J.; Kuhnle, F. N. M. *Tetrahedron Lett.* **1997**, *38*, 8631−8634.
(20) Tokunaga, M.; Larrow, J. F.; Kakiuchi, F.; Jacobsen, E. N. *Science (Washington, DC)* **1997**, *277*, 936−938.

JA0387554